PAPER

NJC

www.rsc.org/njc

Template extraction from surface-functionalised zeolite β nanoparticles

Béatrice Gautier and Monique Smaïhi*

Institut Européen des Membranes (UMR 5635, CNRS-ENSCM-UM2), CNRS, 1919 route de Mende, 34293, Montpellier cedex 5, France. E-mail: smaihi@iemm.univ-montp2.fr; Fax: +33 4 6704 2820; Tel: +33 4 6761 3393

***Received* (in Montpellier, France) 7th November 2003, Accepted 26th November 2003**
First published as an Advance Article on the web 24th February 2004

Colloidal suspensions of functionalised zeolite nanoparticles have been prepared by a two-step procedure. Organic ligands were grafted to the surface of the zeolite nanoparticles, playing the role of functionalising groups as well as protective groups against framework alteration during subsequent solvent extraction of the structure directing agent (SDA). The effect of each step of the preparation procedure on particle size, morphology, crystallinity and the microporous properties of the material was studied by XRD, DLS, SEM and N_2 adsorption measurements. Nanoparticle surface bonding has been investigated by ^{29}Si and ^{31}P MAS NMR. The accessibility and stability of the anchored functional groups on the final materials has been proved by fluorescence spectroscopy. This preparation procedure allows the size, morphology and crystallinity of the initial zeolite nanoparticles to be preserved, while opening the microporosity and modifying their surface reactivity.

Introduction

Functionalised nanoparticles already play an important role in many technologies, for example in paint dispersion, catalyst optimisation and in processes involving adhesives, biocements, varnishes and lubricants.[1] Organically functionalised metal oxide nanoparticles allow one to design a large variety of new hybrid materials and devices.[1,2] In particular, multiscale ordering of functional colloidal nanoparticles is a powerful technique for the creation of macroscopic devices.[3–7] Among inorganic materials, the synthesis and studies of nanosized zeolites have attracted considerable attention in the last decade.[8–14] The tuneable chemical composition of zeolite frameworks makes zeolite nanocrystals attractive supports for organic functionalisation. Recently, self-assembly of zeolite nanocrystals has been achieved to produce three-dimensional objects that could lead to applications such as controlled release capsules, artificial cells, chemical sensors and adsorbents.[15] However, zeolite nanoparticles synthesised in the form of a stable colloidal suspension[8–13] usually contain an organic structure directing agent (SDA) in the intracrystalline voids. This SDA has to be removed to take advantage of the zeolite microporosity. The most commonly used method for template removal is through high temperature calcination in air or oxygen. This method, however, was found to be unsuitable for colloidal nanocrystals because it led to significant irreversible aggregation.[16,17] In addition, the calcination procedure would destroy any previous grafted organic molecules. Mild solvent extraction is one of the preferred methods for SDA removal from mesoporous solids.[18] For microporous materials, specifically zeolites, solvent extraction is less used because complete extraction of the SDA molecules is often impossible. In addition, this chemical treatment could damage the zeolite framework.[19] Therefore, methods that might open at least a part of the zeolite porosity without alteration of the framework and grafted organic ligands are highly desired.

Among the solid surface modifications available, organothiols remain the most popular compounds for metal surfaces.[20] Surface modification of metal oxides (SiO_2,[21,22] Al_2O_3, Fe_2O_3, TiO_2,[23] ZrO_2,[24] *etc.*) has also been developed. Although organosilanes are widely used for the functionalisation of various oxides, there are inconveniences in their application.[1,25,26] The major drawback in functionalisation with organosilanes is homocondensation in the presence of traces of water, which may lead to multilayers or even gel formation instead of condensation at the surface. Organophosphorous compounds offer a promising alternative in the coupling of organic components to metal oxides. The reactivity of organophosphorous coupling molecules appears to be quite different from that of organosilane coupling agents. Homocondensation with the formation of P–O–P bridges is unlikely and such bridges would not be stable in the presence of water. Recent studies dealing with the anchoring chemistry of phosphonic acids with oxide surfaces showed that the anchoring involves both the coordination of the phosphoryl oxygen to Lewis acid sites and the condensation of P–OH groups with surface M–OH hydroxyl groups.[23,24,27,28] In the present study we have employed the phosphonic acid methodology, seldom reported for the grafting of microporous zeolite-type materials,[29] in order to functionalise zeolite nanocrystals. It is worth mentioning that organosilanes and phosphonic acids are complementary coupling agents. Their different chemical reactivities can be used to control surface modification, thus providing opportunities to obtain a dispersed functionality up to a well-packed monolayer.

In the present work, we report a novel approach to prepare colloidal suspensions of functionalised microporous zeolite nanoparticles where the organic ligands, grafted on the surface of the zeolite nanoparticles prior to SDA extraction, protect the inorganic framework from alteration and aggregation while remaining intact in the final material.

Results and discussion

The surface of colloidal zeolite β crystals (Si:Al ratio of 15.5) have been functionalised by treatment with an alcoholic solution of aminoethylphosphonic acid (APA) or an

DOI: 10.1039/b314298a

aminopropyltriethoxysilane (APTS). Regardless to the coupling agent used, stable suspensions were obtained. Subsequently, extraction of tetraethylammonium hydroxide (TEA) from the hybrid material was effectuated by solvent extraction in aqueous acetic acid. The different stages of the preparation procedure are summarized in the flowchart diagram (Scheme 1).

Particle size, morphology and crystallinity

A dynamic light scattering (DLS) study has been performed at each step of the preparation procedure. Zeolite β particles with similar diameter and particle size distributions were recorded before and after grafting and after the final extraction procedure (Table 1, Fig. 1). This is serious proof that the functionalisation of the particles does not provoke uncontrolled aggregation. SEM analysis of the samples confirmed that there are no morphological differences between the as-prepared and treated samples. Powder X-ray diffraction analyses were performed on the as-synthesized nanoparticles, the grafted nanoparticles and the extracted powder. According to XRD analyses, as-synthesized and treated samples have similar crystallinities (Fig. 2). These results show that, regardless of the coupling molecule used, the grafting and extraction processing did not provoke substantial changes in the size, morphology and crystallinity of the zeolite nanoparticles.

Nature and quantification of the grafting

^{29}Si and ^{31}P MAS NMR was performed on the samples at each step of the preparation procedure in order to characterise the surface bonding. Fig. 3 shows the ^{29}Si cross-polarisation magic angle spinning (CP-MAS) NMR spectra for the silane-functionalised zeolite before and after extraction. Around −110 ppm, the overlapping resonances for all the samples are assigned to zeolite framework silicon atoms. Resonances around −113/−115 ppm and −109/−110 ppm are assigned to $Si(OSi)_4$ species with minor resolution of the crystallographic sites. The signal at −100 ppm is assigned to $Si(OSi)_3OH$ species. The presence of a signal between −60 and −70 ppm indicates that the aminosilane group is covalently linked to the zeolite framework silicon atoms and that the extraction procedure did not remove the grafted organic group. Two resonances are observed corresponding to Si attached to the organic chain in two different chemical environments [−67 ppm: C–Si–$(OSi)_3$ and −60 ppm: C–Si–$(OSi)_2OH$ species]. The extraction procedure provokes a decrease of the signal intensity at −60 ppm. This effect can be attributed to the reflux treatment, which may induce a condensation of the C–Si–$(OSi)_2OH$ species into C–Si–$(OSi)_3$. Fig. 4 displays the ^{31}P high-power decoupling (HPDEC) NMR spectra of the aminoalkylphosphonic acid (APA) and the phosphonate-functionalised zeolite after extraction. The ^{31}P NMR spectrum is considerably broadened upon reaction with zeolite nanoparticles. The spectrum presents a sharp signal at 19.4 ppm (identical to the APA resonance) assigned to phosphonic acid groups that are weakly interacting with the surface *via* hydrogen bonding interactions. The signal at 13.4 ppm is assigned to phosphonate groups bonded to the zeolite surface. The large line width arises from a distribution of binding sites and bonding modes of the POH headgroup on the zeolite surface.

Elemental analysis enables the quantification of the organic species grafted at the nanoparticle surface before and after the extraction procedure. (Table 1). The average number of coupling molecules suggests a coverage not exceeding a monolayer in all cases. Before SDA removal, the concentration of silane grafting is about 250 μmol g^{-1} while for the phosphonate grafted material it is about 161 μmol g^{-1} The solvent extraction procedure does not modify the APTS coverage while the APA grafting is greatly decreased. This decrease is attributed to the removal of a part of the hydrogen-bonded phosphonate groups (observed in the NMR spectra) by the acidic water treatment of the particles. In contrast, the silica species (APTS) grafted on the zeolite surface are not removed upon solvent treatment.

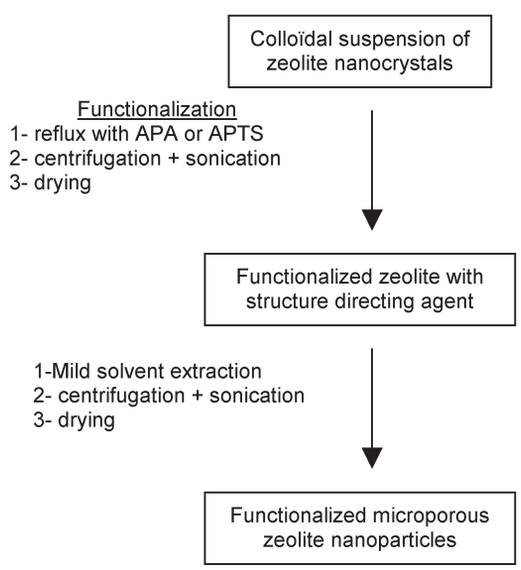

Scheme 1 Preparation procedure for amine-functionalised zeolite nanoparticles.

Microporosity

In order to follow the influence of the various treatments on the porous characteristics of the samples, nitrogen gas sorption analyses were performed on the as-synthesized nanoparticles, the grafted nanoparticles and the extracted powder. Grafting of the zeolite nanoparticles, regardless of the coupling molecule used, did not change drastically the specific surface area of the as-synthesized sample (Table 1). The zeolite microporosity is revealed by N_2 adsorption (0.12 cm^3 g^{-1}) and the specific

Table 1 Chemical, textural and morphological characteristics of the zeolite nanoparticles as a function of the grafting and extraction steps

	Elemental analysis			Porosity		
	Si:Al	TEA per unit cell	APA (APTS)/ μmol g^{-1}	BET area/ m^2 g^{-1}	Micropore volume/ cm^3 g^{-1}	Crystal size (± 5%)/nm
As-synthesized nanoparticles	15.5	6	0	221	0	153
APTS-grafted nanoparticles	15.9	6.1	250	162	0	162
APA-grafted nanoparticles	15.3	5.8	161	235	0	145
Extracted APTS-grafted nanoparticles		2.4	250	301	0.12	180
Extracted APA-grafted nanoparticles	15.4	1.8	60	332	0.12	172
Calcined zeolite β	Not meas.	0	0	476	0.2	275

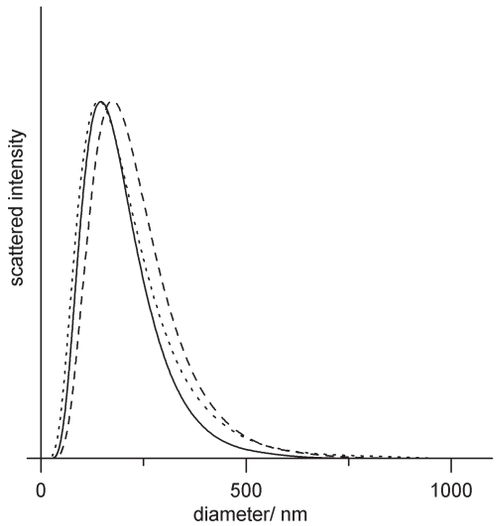

Fig. 1 DLS data of (full line) as-synthesized zeolite nanoparticles, (dotted line) APTS-functionalised nanoparticles and (dashed line) SDA-extracted APTS-functionalised nanoparticles.

surface area is slightly increased ($\sim$330 m^2 g^{-1}) after extraction (Table 1). This micropore volume corresponds to 60% of the micropore volume of a calcined sample. This estimation is in good agreement with the elemental analysis, which showed that the number of TEA molecules per unit cell is $\sim$2.1, which is approximately 65% of the 6 TEA molecules in the unit cell of the as-synthesized material. The yield of solvent extraction depends on both the size of the SDA relative to the size of the micropore and the strength of the interaction between the SDA and the framework.[12] Concerning zeolite β (with Si:Al $\sim$ 15), it has been shown that the limit of SDA solvent extraction is around 60% of the TEA per unit cell. The above results show that pre-functionalisation does not modify the extraction limit. It is worth mentioning that the Si:Al ratio is almost constant during this procedure, which confirms that functionalising before extracting prevents alteration of the framework (Table 1).

Functionalisation

The accessibility and stability of the primary amino groups grafted on the zeolite nanoparticle surfaces was investigated by fluorescence spectroscopy using (2-furoyl) quinoline-2-carboxyaldehyde (Atto TAG FQ, Molecular Probes, Leiden, The Netherlands). This substance, intrinsically non-fluorescent, binds selectively to primary amino groups, resulting in a fluorescent complex with an excitation wavelength of 480 nm and an emission wavelength of 590 nm. It has proven to be an extremely sensitive reagent capable of detecting very low concentrations of amino groups.[30,31]

No fluorescence was observed for as-synthesised zeolite nanoparticles, while intense emission spectra were obtained for functionalised colloids (Fig. 5). No drastic changes in the emission spectra were observed after SDA extraction, which proved that the primary amino groups were still present on the nanoparticle surfaces after the extraction procedure. A slight shift of the fluorescence maximum was observed after extraction, which could be attributed to a decrease in the amine group concentration.

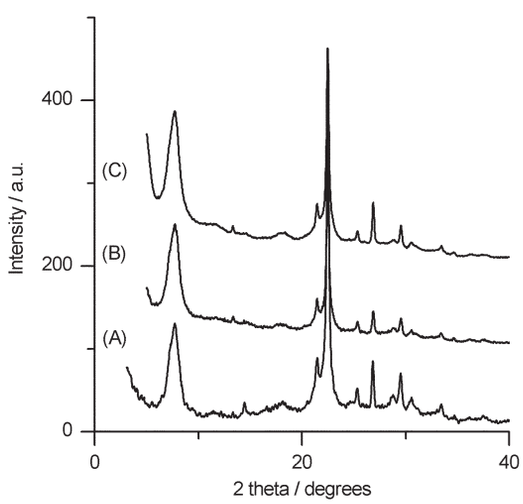

Fig. 2 XRD patterns of (A) as-synthesized zeolite nanoparticles, (B) APTS-functionalised nanoparticles and (C) solvent-extracted APTS-functionalised nanoparticles.

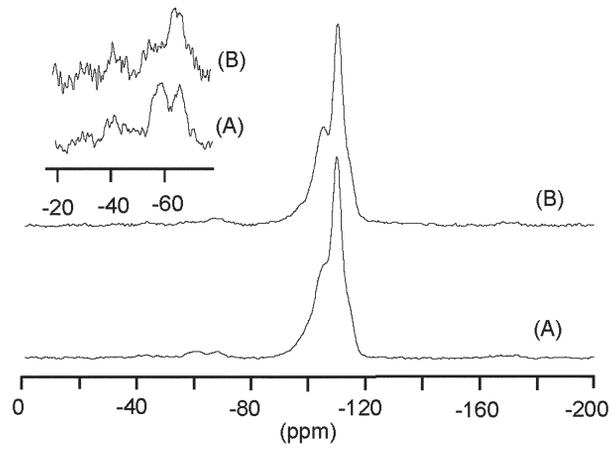

Fig. 3 ^{29}Si CP-MAS NMR spectra of (A) APTS-functionalised zeolite nanoparticles and (B) SDA-extracted APTS-functionalised zeolite nanoparticles.

Conclusion

We have demonstrated that a substantial part of the organic template in functionalised colloidal zeolite nanoparticles can be extracted *via* a mild solvent extraction that leaves intact the organic ligands attached to the surface of the zeolite nanoparticles. The developed synthetic approach was exemplified by grafting of aminoethylphosphonic acid (APA) and aminopropyltriethoxysilane (APTS). Nanoparticle surface bonding

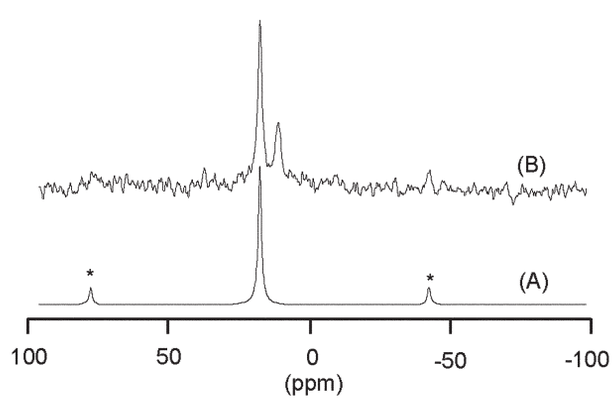

Fig. 4 ^{31}P HPDEC NMR spectra of (A) APA and (B) SDA-extracted APA-functionalised zeolite nanoparticles (* mark the spinning side bands).

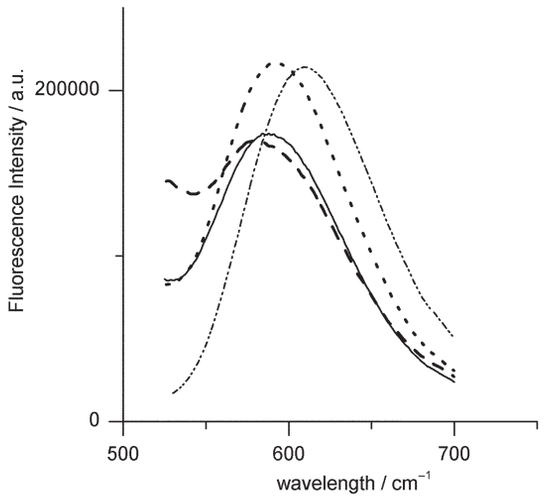

Fig. 5 Emission fluorescence spectra of (dotted lined) APTS-functionalised nanoparticles, (dashed-dotted line) APA-functionalised nanoparticles, (dashed line) SDA-extracted APA-functionalised nanoparticles and (full line) SDA-extracted APTS-functionalised nanoparticles

has been demonstrated by ^{29}Si and ^{31}P MAS NMR. The grafting and subsequent extraction processing has no influence on the size, morphology and crystallinity of the zeolite nanoparticles. The mild solvent SDA extraction procedure has opened about 65% of the as-synthesized zeolite β microporosity. The accessibility and stability of the anchored functional groups on the final materials has been attested by fluorescence spectroscopy.

This approach is applicable to frameworks where the size of the SDA is smaller than the size of the largest micropore of the solid (*i.e.*, BEA and MFI topology with TEA-based SDAs).[32] It opens up new routes for the preparation of various functional materials. The aminoalkyl groups should allow immobilisation of a variety of groups on colloidal zeolites through the amine functionality. Moreover, this surface modification enables the dispersion of these colloidal particles in various organic solvents like DMSO, DMF, alcohols, *etc.* and thus extends the use of microporous inorganic particles in organic medium. This approach might also be used for the construction of hierarchical inorganic-organic hybrid materials using these particles as building blocks.

Experimental

Materials preparation

Colloidal zeolite β crystals with a Si:Al ratio of 15.5 were synthesised under mild hydrothermal conditions from a clear solution containing 0.28 Na_2O:9.0 $(TEA)_2O$:0.5 Al_2O_3:25 SiO_2:430 H_2O, where TEA is tetraethylammonium hydroxide (Fluka, 20% in water). The synthesis was performed at 100 °C for 8 days. The colloidal zeolite β crystals were purified by a series of high speed centrifugations and re-dispersion in water or ethanol. The obtained colloidal suspensions were adjusted to a 4 wt % concentration. An aminoethylphosphonic acid [APA; $H_2N(CH_2)_3POOH$, Fluka] or an aminopropyltriethoxysilane [APTS; $H_2N(CH_2)_3Si(OC_2H_5)_3$, ABCR] were used for the preparation of the surface-modified nanoparticles in a 4-fold excess relative to the amount needed for full surface coverage on the particles. Typically, an alcoholic solution of APA or APTS (0.125 g APA in 10 ml ethanol or 0.221 g APTS in 1 ml ethanol) was added to the zeolite nanoparticle suspension (1 g of nanoparticles) and stirred under reflux (80 °C) for 12 h. The organic reagent:zeolite particle ratio was fixed at 1 mmol g^{-1}. After the reaction, the excess of reagent was eliminated by repeated centrifugation (12 000 rpm) and re-dispersion by ultrasonication. The recovered solid was dried at 80–100 °C overnight. Subsequently, extraction of TEA from the hybrid material was effectuated by exposure of the solid powder to aqueous acetic acid (50% water) at 80 °C for 12 h.[19] After this treatment, the solid was washed by repeated centrifugation (3 times, 12 000 rpm) and re-dispersion by ultrasonication. A dispersible white powder was obtained after drying at 80–100 °C overnight.

Sample characterisation

Scanning electron micrographs were obtained on a HitachiS-4500 microscope. All samples were platinum coated (2–3 nm) and mounted on aluminium mounts with carbon conducting tape. X-Ray diffraction measurements were performed with a Bruker D-5000 diffractometer (Cu Kα_1 radiation = 0.154 nm). ^{29}Si CP-MAS NMR spectra of the solid samples were recorded on a Bruker spectrometer at 79.49 MHz using 5 μs single pulses (60° flip angle) with 10 s repetition rate and 5 ms contact time, employing magic angle spinning at 3.5 kHz; 10 000 scans were accumulated. ^{31}P MAS NMR spectra were obtained at 161.98 MHz using single pulses of 4 μs duration (45° flip angle) with a 60 s repetition rate, employing high power proton decoupling and magic angle spinning at 10 kHz; 512 scans were accumulated. The powder samples were filled into 4 mm diameter zirconia rotors. All ^{31}P and ^{29}Si chemical shifts were referenced to H_3PO_4 solution (85% in water) and tetramethylsilane (TMS), respectively.

Dynamic light scattering (DLS) results were obtained using an He-Ne laser (10 mW) operating at 633 nm. Light scattering measurements were made at 25 ± 0.1 °C.

Fluorescence spectra were registered on a Spex Fluorolog 1681 spectrometer (scanning rate 2 nm s^{-1}). Appropriate filters were used to eliminate Rayleigh and Raman scatters from the emission. The derivatisation was carried out following the protocol proposed by Molecular Probes. Typically, the derivatisation is carried out by mixing 50 μL of a solution of the dispersed functionalised zeolite (1 mM in 100 mM sodium borate buffer, pH 9.3) with 50 μL of 10 mM KCN aqueous solution and 50 μL of 10 mM Atto TAG EtOH solution. This mixture is allowed to react for 5 h at room temperature. Finally, 1.85 mL sodium borate buffer is added to obtain a 2 mL sample for the fluorescence experiments.

Gas sorption experiments were performed by using a Micromeretics ASAP 2010. Nitrogen was used as the adsorbate at 77 K. The micropore volume was determined by the T-plot method. Samples were outgassed at 150 °C in dynamic vacuum (3×10^{-6} bar) before the adsorption. This outgassing treatment, selected upon considering the thermogravimetric results, does not remove the organics from the sample.

Elemental analysis were done by the "Laboratoire Central d'Analyses du CNRS" at Vernaison (France).

Acknowledgements

The authors thank Drs. V. Valtchev and H. Kessler (LMM, Mulhouse) and Dr. J.-O. Durand (LCMOS, Montpellier) for helpful discussions.

References

1 C. Sanchez, G. J. de A. A. Soler-Illia, F. Ribot, T. Lalot, C. R. Mayer and V. Cabuil, *Chem. Mater.*, 2001, **13**, 3061.
2 A. Bouchara, G. J. de A. A. Soler-Illia, J.-Y. Chane-Ching and C. Sanchez, *Chem. Commun.*, 2002, 1234.
3 H. Cölfen and S. Mann, *Angew. Chem. ,Int. Ed.*, 2003, **42**, 2350.
4 M. Davis, *Nature (London)*, 2002, **417**, 813.
5 H. Zhang, G. C. Hardy, M. J. Rosseinsky and A. I. Cooper, *Adv. Mater.*, 2003, **15**, 78.

6 L. M. Huang, Z. B. Wang, J. Y. Sun, L. Miao, Q. Z. Li, Y. Yan and D. Y. Zao, *J. Am. Chem. Soc.*, 2000, **122**, 3530.
7 O. D. Velev and E. W. Kaler, *Adv. Mater.*, 2000, **12**, 531–534.
8 B. J. Schoeman, J. Sterte and J.-E. Otterstedt, *Zeolites*, 1994, **14**, 110.
9 A. E. Persson, B. J. Schoeman, J. Sterte and J.-E. Otterstedt, *Zeolites*, 1994, **14**, 557.
10 M. Tsapatsis, M. Lovallo, T. Okubo and M. E. Davis, *Mater. Res. Soc. Symp. Proc.*, 1995, **371**, 21.
11 M. A. Camblor, A. Corma, A. Misud, J. Perez-Pariente and S. Valencia, in *Progress in Zeolites Microporous Materials, Proceedings of the 11th IZC*, eds. H. Chon, S.-K. Ihm and Y. S. Uh, 1996; M. A. Camblor, A. Corma, A. Misud, J. Perez-Pariente, S. Valencia, *Stud. Surf. Sci. Catal., A*, 1996, **105**, 341.
12 J.-P. Dong, J. Zou and Y.-C. Long, *Microporous Mesoporous Mater.*, 2003, **57**, 9.
13 A. Kulak, Y. J. Lee, Y. S. Park, H. S. Kim, G. S. Lee and K. B. Yoon, *Adv. Mater.*, 2002, **14**, 526.
14 L. Tosheva, B. Mihailova, V. Valtchev and J. Sterte, *Microporous Mesoporous Mater.*, 2000, **39**, 91.
15 M. J. MacLachlan, I. Manners and G. A. Ozin, *Adv. Mater.*, 2000, **12**, 675.
16 L. M. Huang, Z. B. Wang, J. Y. Sun, L. Miao, Q. Z. Li, Y. Yan and D. Y. Zha, *J. Am. Chem. Soc.*, 2000, **122**, 3530.
17 B. J. Zhao, S. A. Davis, N. H. Mendelson and S. Mann, *Chem. Commun.*, 2000, 781.
18 T. Asefa, M. J. MacLachlan, N. Coombs and G. A. Ozin, *Nature (London)*, 1999, **402**, 867.
19 C. W. Jones, K. Tsuji, T. Takewaki, L. W. Beck and M. E. Davis, *Micoporous Mesoporous Mater.*, 2001, **48**, 57.
20 D. Zanchet, C. M. Micheel, W. J. Parak, D. Gerion and A. P. Alivisatos, *Nano Lett.*, 2001, **1**, 32.
21 I. Lukěs, M. Borbaruah and L. D. Quin, *J. Am. Chem. Soc.*, 1994, **116**, 1737.
22 R. D. Badley, W. T. Ford, F. J. McEnroe and R. A. Assink, *Langmuir*, 1990, **6**, 792.
23 G. Guerrero, P. H. Mutin and A. Vioux, *Chem. Mater.*, 2001, **13**, 4367.
24 S. Pawsey, K. Yach and L. Reven, *Langmuir*, 2002, **18**, 5205.
25 K. C. Vranken, K. P. Possemiers, P. Van der Voort and E. F. Vansant, *Colloids Surf., A*, 1995, **98**, 235.
26 A. Stein, B. J. Melde and R. C. Schroden, *Adv. Mater.*, 2000, **12**, 1403.
27 C. Carbonneau, R. Frantz, J.-O. Durand, M. Granier, G. F. Lanneau and R. J. P. Corriu, *New J. Chem.*, 2001, **25**, 1398.
28 R. Duval and J. C. Yvin, Patent FR 2773172-A1, 1997.
29 L. D. Quin, M. Borbaruah, G. S. Quin, L. C. Dickinson and S. Jankowski, *Heteroatom Chem.*, 1998, **9**, 691.
30 S. C. Beale, Y.-Z. Hsieh, D. Wiesler and M. Novotny, *J. Chromatogr.*, 1990, **499**, 579.
31 J. Liu, Y.-Z. Hsieh, D. Wiesler and M. Novotny, *Anal. Chem.*, 1991, **63**, 408.
32 H. Lee, S. I. Zones and M. E. Davis, *Nature (London)*, 2003, **425**, 385.